

CHARACTERIZATION OF LANDSLIDES ON MARS AND IMPLICATIONS FOR POSSIBLE FAILURE MECHANISMS.

Donald M. Hooper and Kevin J. Smart. Geosciences and Engineering Division, Southwest Research Institute[®], 6220 Culebra Road, San Antonio, TX 78238-5166 (dhooper@swri.org and ksmart@swri.org).

Introduction: On Mars, the main scarp and displaced material of a Valles Marineris landslide provide insight into possible failure mechanisms and the mechanical nature of the surface and shallow subsurface of the planet. Valles Marineris, the vast equatorial trough system on Mars, is a complex tectonic feature with its formation coupled to the tectonic, magmatic, and geodynamic history of the adjacent Tharsis region [1]. The depth of some Valles Marineris troughs is as much as 11 km below the surface of the surrounding plateau [2]. The absence of recent vigorous fluvial erosion and pluvial activity to infill these depressions is the inferred cause of such astounding relief [3,4]. Canyon (chasma) walls can be divided into two major morphological types: segments displaying landslide scars and segments characterized by spur-and-gully topography.

Canyon Wall Morphology: The canyon walls of the Valles Marineris troughs are characterized by horizontal layering and topped by a pervasive cap rock. High-resolution image data typically show a 750-m- to 1-km-high steep slope along the uppermost walls at the plateau edge (Fig. 1). Beneath this cliff-forming unit, a mantle of talus (and dust) partially obscures canyon slopes. Horizontal layering is evident by exposures of protruding, competent layers within the canyon slopes. However, the spur-and-gully topography, with its bifurcating character and talus cover, make it difficult to correlate resistant layers from one exposure to another. Horizontal layering has been identified at depths of at least 8 km within the canyons [5]. The layered strata are similar to terrestrial flood basalts because their thicknesses and cliff-forming topography are consistent with such volcanic flows and their spectral properties indicate mafic glass and pyroxene [5]. A more recent study concluded that no proper sedimentary layers were observed within the walls of Valles Marineris at the resolution available today, and that old Noachian lava flows and other remnants of the primitive crust can be identified in the deepest exposures of the canyon system [6]. Rock Mass Rating system measurements for Valles Marineris wallrock are consistent with layered igneous rock [7]. However, we point out that the overall wall strength may be controlled by sequences of strong layers with steep slopes; consequently, the majority of the layers could be much weaker, perhaps composed of volcanoclastic sediments or welded tuff [8–11].

Spur-and-gully topography is a distinguishing attribute of canyon walls. Common slope maps drawn across representative segments of both north and south walls of Ius and Coprates Chasmata have mean slope angles ranging between 19° and 23°. These slope angles are less than the massive talus-dominated scarps associated with large Martian landslides, which typically have mean slope angles ranging between 27° and 32° [12]. Gully formation throughout Valles Marineris predates the large landslides, whose scarps and deposits of displaced material generally obliterate and erase spur-and-gully topographies. Straight cliffs, which we interpret to be fault scarps, truncate the spur-and-gully topography near the base of several canyon walls.

Martian Landslides: Large landslides within Valles Marineris form arcuate to straight, slab-like re-entrants in the canyon walls. Local recession of the main scarp may reach or exceed 10 km from the adjacent canyon walls for alcoves within Ius and Ophir Chasmata. The main scarps from these landslides are massive and talus covered, with a smooth to narrowly-ribbed appearance. Using a subset of the largest landslides in Valles Marineris, the average vertical drop from the top of the landslide scarp to the floor of the canyon is approximately 6 km [13]. These landslides typically have displaced and rotated (slump) blocks of competent strata at their heads, which generally do not extend far beyond the re-entrant [4]. The failure surface may be related to changes in mechanical wallrock properties as well as permafrost or aquifer depth.

Martian landslides can be either confined by canyon walls or unconfined. When unconfined, maximum runout distances across the canyon floors have been measured to be approximately 80 km. Both types of landslides have transverse ridges. By using measurements of mean slope angle and topographic texture (standard deviation of elevation) for both the main scarp and the displaced material, we previously demonstrated in a quantitative manner the morphometric distinction between confined and unconfined landslides [12]. Confined landslides have a more rugged surface morphology.

Unconfined landslides may exhibit a longitudinal pattern of ridges and furrows below either the transversely ridged and hummocky material or the displaced blocks [3]. In some instances, the longitudinal ridges and furrows may widen during flow and may become curved as the displaced material fans out. For other

landslides the pattern may remain more uniform. The longitudinal pattern is noteworthy because these are rarely seen in terrestrial landslides, which generally have transverse ridges. The exception is for landslides traveling over the surface of a glacier and in particular the 1964 Alaskan landslide that moved over the Sherman glacier following a strong earthquake [14]. Longitudinal grooves in the Sherman landslide can result from shearing between rapidly moving debris traveling forward at slightly different speeds or times [14]. A high velocity is inferred. De Blasio [15] noted that not all landslides traveling on glaciers develop furrows. He suggested that the natural lubricant for landslides in Valles Marineris was either ice, deep water (e.g., lakes), a shallow water layer, or evaporites [15].

Landslides in Valles Marineris occur adjacent to prominent normal-fault scarps that bound the troughs [4]. Schultz [7] concluded that in the absence of factors affecting pore-pressure—such as rainfall or snow-melt—seismic slip along these trough-bounding normal faults is considered the most plausible mechanism for triggering landslides in wallrock. Our observation of morphologic indicators, including the truncation of spur-and-gully topography by normal faults, supports this conclusion. Additionally, our discrete element models simulated the effects of faulting on slope failure in Valles Marineris and support faulting as a triggering mechanism for landslide initiation [11].

Conclusion: We conclude that the following features infer the present or past occurrence of volatiles in Valles Marineris wallslopes at the time of landslide emplacement: spur-and-gully topography, lobate shape of some landslide debris aprons, longitudinal pattern observed on some debris aprons, tributary canyons formed by groundwater sapping (Fig. 1), long runout distances or mobility, volume deficit of landslide deposits [13], and “wet” debris flows [16]. However, McEwen [17] concluded that many features of landslides within Valles Marineris are analogous to dry terrestrial rock avalanches and Jernsletten [18] concluded that ground ice did not play a role in initiating or mobilizing these landslides. Therefore, the overall role of water or other volatiles in the dynamics of landslide emplacement on Mars remains controversial.

Acknowledgments: This work was supported by NASA MDAP grant #NNX09AI44G. The authors thank Danielle Wyrick and Gary Walter for constructive reviews.

References: [1] Andrews-Hanna J. C. (2012) *J. Geophys. Res.*, 117, E06002, doi:10.1029/2012JE004059. [2] Lucchitta B. K. et al. (1994) *J. Geophys. Res.* 99(E2), 3783–3798. [3] Lucchitta B. K. (1979) *J. Geophys. Res.* 84, 8097–8113. [4] Lucchitta B. K. et al. (1992) *In: Kiefer H. H.*

et al. (Eds.), *Mars*. Univ. of Arizona Press, pp. 453–492. [5] McEwen A. S. et al. (1999) *Nature* 397, 584–586. [6] Flahaut J. et al. (2012) *Icarus* 221, 420–435. [7] Schultz R. A. (2002) *Geophys. Res. Lett.* 29(19), 1932. [8] Beyer R. A. and McEwen A. S. (2005) *Icarus* 179, 1–23. [9] Sims D.W. et al. (2008) *Eos Trans. AGU*, 89(53), Abstract P33B-1448. [10] Smart K. J. et al. (2010) AGU Fall Meeting, Abstract P51B-1430. [11] Smart K. J. and Hooper D. M. (2013) This conference. [12] Hooper D.M. and Smart K. J. (2012) *LPSC 43*, Abstract #2323. [13] Quantin C. et al. (2004) *Planet. Space Sci.* 52, 1011–1022. [14] Shreve R.L. (1966) *Science* 154, 1639–1643. [15] De Blasio F. V. (2011) *Planet. Space Sci.* 59, 1384–1392. [16] Lucchitta B. K. (1987) *Icarus* 72, 411–429. [17] McEwen A. S. (1989) *Geology* 17, 1111–1114. [18] Jernsletten J. A. (2004) *J. Geophys. Res.* 109, E12004, doi:10.1029/2004JE002272.

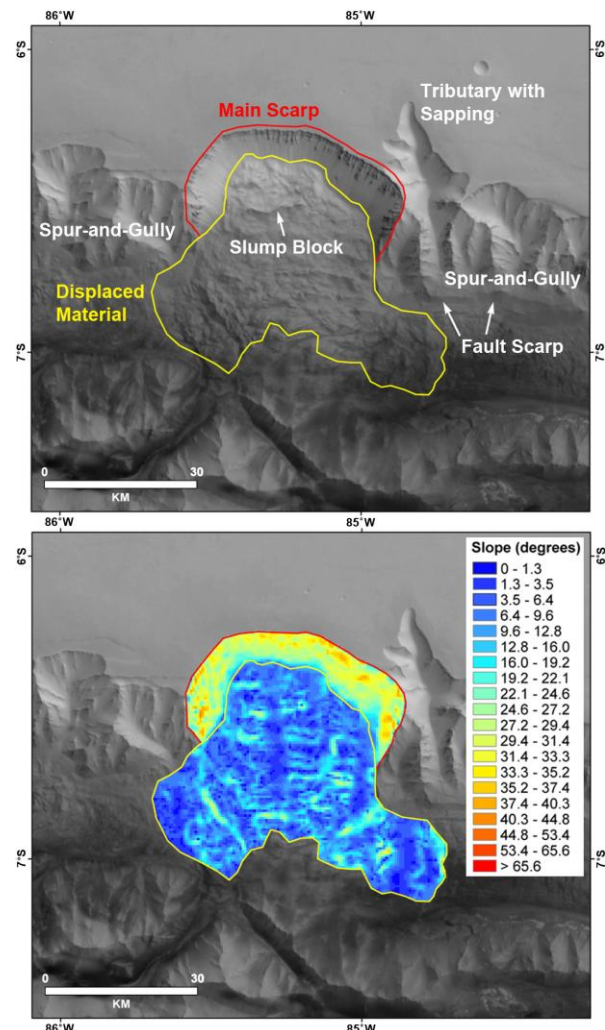


Figure 1. HRSC (High-Resolution Stereo Camera) image and slope map of a landslide in Ius Chasma.